Title	T dependence of nuclear spin-echo decay at low temperatures in $YbRh_2Si_2$
Author(s)	Kambe Shinsaku, Sakai Hironori, Tokunaga Yo, Hattori Taisuke, Lapertot G., Matsuda Tatsuma, Knebel G., Flouquet J., Walstedt R. E.
Citation	Physical Review B, 95(19), p.195121_1-195121_8
Text Version	Publisher's Version
URL	https://jopss.jaea.go.jp/search/servlet/search?5059331
DOI	https://doi.org/10.1103/PhysRevB.95.195121
Right	©2017 American Physical Society

T dependence of nuclear spin-echo decay at low temperatures in $YbRh_2Si_2$

S. Kambe,[1] H. Sakai,[1] Y. Tokunaga,[1] T. Hattori,[1] G. Lapertot,[2] T. D. Matsuda,[1,*] G. Knebel,[2] J. Flouquet,[2] and R. E. Walstedt[3]

[1]*Advanced Science Research Center, Japan Atomic Energy Agency, Tokai-mura, Ibaraki 319-1195, Japan*

[2]*Institut Nanosciences et Cryogénie, CEA-Grenoble/Université J. Fourier Grenoble I, 17 rue des Martyrs 38054 Grenoble, France*

[3]*Physics Department, The University of Michigan, Ann Arbor, Michigan 48109, USA*

(Received 31 December 2016; revised manuscript received 13 April 2017; published 10 May 2017)

The authors report ^{29}Si nuclear spin-echo oscillations and decay measurements on a single crystal of $YbRh_2Si_2$. These quantities are found to be T independent from 300 K down to ~20 K, showing, however, a strong T dependence below 20 K. These results indicate that electronic states near the Fermi level are modified at low temperatures. The observed spin-echo oscillations can be interpreted with the Ruderman-Kittel and pseudodipolar interactions between nearest-neighbor Si nuclei driven by conduction electron scattering at the Fermi surface. Possible modifications to the Fermi surface at low temperatures are discussed.

DOI: 10.1103/PhysRevB.95.195121

I. INTRODUCTION

The field-induced quantum critical phase transition (QCPT) in $YbRh_2Si_2$ at a critical field H_c is not the usual case of spin-density wave instability observed in Ce-based compounds [1,2], but instead is a candidate for the locally critical QCPT case [3–5]. A strong-coupling model has also been proposed to be relevant [6]. A sudden change of Fermi-surface volume has been suggested theoretically [5] in the vicinity of the locally critical QCPT. In fact such a change of Fermi surface has also been suggested by transport measurements [7–10]. In addition, the Fermi surface is easily modified under magnetic field far above H_c through a Lifshitz-type transition [11–14]. Furthermore, the electronic properties are quite sensitive to the valence of Yb [15,16]. Recent angle-resolved photoemission spectroscopy (ARPES) measurements on $YbRh_2Si_2$ indicated no drastic change of Fermi surface near the QCPT with decreasing temperature down to 1 K [17]. In contrast, heavy quasiparticle formation with change of Fermi surface was observed below 50 K in ARPES measurements using a laser photon source [18]. As described above, the precise nature of the Fermi surface of $YbRh_2Si_2$ remains controversial.

In our previous papers [19,20], coexisting static Fermi-liquid (FL) and non-Fermi-liquid (NFL) states near the QCPT in $YbRh_2Si_2$ were brought to light by means of ^{29}Si nuclear spin-lattice relaxation time (T_1) studies with $H \parallel a$ and c axes. The latter results may be related to localized character and valence instability of $4f$ electrons in $YbRh_2Si_2$.

In the present investigation, ^{29}Si nuclear spin-echo decay and oscillations are measured in $YbRh_2Si_2$ in order to probe changes in the electronic structure as a function of temperature. Observed strong modification of these quantities, especially of oscillations below 20 K, indicates a modification of electronic states at the Fermi level.

Ruderman and Kittel showed that conduction electrons induce an indirect scalar interaction between neighboring nuclear spins in metals. This is now well known as the Ruderman-Kittel (RK) interaction [21]. Subsequently, Bloembergen and Rowland pointed out the existence of a similar pseudodipolar (PD) indirect nuclear spin-spin coupling [22]. At the present time, RK and PD interactions are the only well-established origins for ($I = 1/2$) nuclear spin-echo oscillations in metallic systems. These interactions are known to be sensitive to modifications of electronic states near the Fermi level, since they arise through hyperfine couplings with conduction electrons. In fact, previously observed spin-echo oscillation results have been interpreted based on the RK-PD model, and the character of the Fermi surface has been discussed [23–25]. More recently, a combination of NMR data and direct calculations has been employed to study indirect nuclear spin-spin couplings and the bulk electron states that give rise to them in the topological insulator Bi_2Se_3 [26].

The present results are interpreted in the framework of the RK-PD model, which is considered to be basically correct for heavy fermion systems, whereas the ingredients of indirect nuclear spin-spin coupling may be difficult to identify due to heavy conduction-band formation and the related complex nature of the hyperfine interactions. Tentatively, a possible modification of Fermi surface for the observed T dependence of the spin-echo oscillation frequency is presented in this paper, based on a simplified picture.

By way of introduction, we note that the $YbRh_2Si_2$ lattice presents nearly ideal circumstances for measuring the total spin-spin coupling between nearest-neighbor (NN) ^{29}Si pairs using NMR techniques. The crystal structure of $YbRh_2Si_2$ is shown in Fig. 1. The Si lattice sites in this structure occur in NN pairs—two pairs per unit cell separated by a vector $\vec{R}$ oriented along the c axis—that are rather closer together than second, third, etc., neighbors. As a result, the NN spin-spin couplings play a major role in the ^{29}Si ($I = 1/2$, $\gamma/(2\pi) = 845.77$ Hz/Oe) spin-echo decay process. There are other circumstances that were also key to the success of this investigation. First, the measured ^{29}Si linewidth $\gamma\Delta H/2\pi \sim 9$ kHz reveals a modest level of inhomogeneous line broadening that is evidently a consequence of *disorder*. As will be clear in the technical discussion below, this broadening renders the spin-spin couplings among the ^{29}Si completely static, a condition required for the observation of oscillatory modulation of spin echoes [24].

Second, isotopic enrichment of the ^{29}Si nuclear species not only greatly increases the NMR signal amplitude, but

*Present address: Division of Physics, Tokyo Metropolitan University, Hachioji-shi, Tokyo 192-0397, Japan.

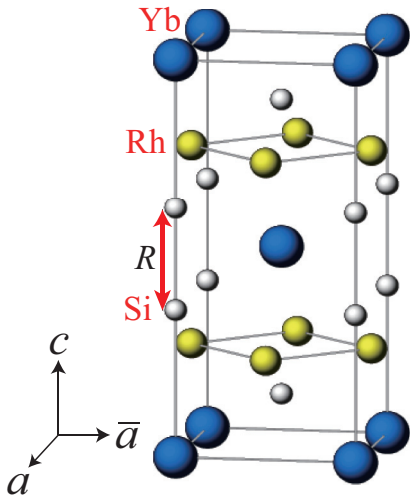

FIG. 1. Crystal structure ($I4/mmm$) of $YbRh_2Si_2$. The nearest neighbors (NNs) among Si sites are indicated by the red arrow with the NN distance $R = r_{01} = 2.39$ Å.

also gives rise to a substantial fraction of ^{29}Si NN pairs that are in this case the sole source of spin-echo oscillations. At a concentration c, the fraction of NN pairs that are both occupied with ^{29}Si is c^2, the fraction that are unoccupied is $(1-c)^2$, and the fraction that is singly occupied is $2c(1-c)$. Thus, the fraction of ^{29}Si which have a NN spin, allowing them to contribute to the spin-echo oscillation amplitude, is simply c, which is 0.52 in the present case. The fraction without a NN spin is therefore $1-c$. Actually, the spin-echo oscillation amplitude is ~10 times smaller in sample with natural abundance of the ^{29}Si, i.e., $c = 0.047$. By measuring the echo oscillation frequency it is possible to monitor the magnitude of their indirect spin-spin couplings and how they vary with temperature. Such measurements reveal significant changes in the electronic state at low temperatures that occur in the vicinity of the QCPT in this system.

II. NMR SPIN-ECHO DECAY

The spin-echo amplitude $m(2\tau)$ decays with increasing time interval τ between the first $(\pi/2)$ and second (π) excitation pulses as a result of nuclear spin-spin interactions (Fig. 2).

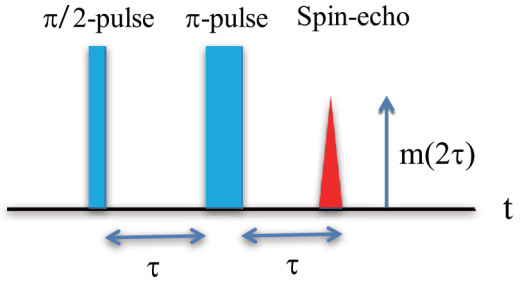

FIG. 2. Schematic description of nuclear spin-echo formation. The $\pi/2$ pulse rotates the nuclear magnetic moments by 90°, the π pulse by 180°.

Generally, the τ dependence of m may be expressed as

$$\frac{m(2\tau)}{m(0)} \approx \exp\left\{-\frac{2\tau}{T_{1L}} - \frac{1}{2}\left(\frac{2\tau}{T_{2G}}\right)^2\right\} \times [f_{\rm non} + f_{\rm osc} W(2\tau)], \quad (1)$$

where $f_{\rm osc} \cong c = 0.52$ and $f_{\rm non} = 1 - f_{\rm osc} \cong 0.48$ are the estimated fractions of the echo signal that do and do not oscillate, respectively, during the echo decay. Also, $2\tau/T_{1L}$ is an exponential relaxation term in the exponent, represented here by spin-lattice relaxation time T_1 data from previous studies [19,20,27]. T_{2G} is a Gaussian model spin-spin relaxation time, which approximately represents the collective relaxation effect of ^{29}Si beyond the first neighbor shell. $W(2\tau)$ is a fractionally oscillatory echo-modulation factor which is the main focus of our study. See Sec. V for more details.

As shown in Fig. 1, there is a single NN site for each Si. (In a previous paper [28] a case with four NN sites was erroneously discussed for this system.) Consistent with the RK-PD model (see Sec. V A) for the single NN site case, $W(2\tau)$ is well fitted in the present case with a single oscillation frequency $G_{a,c}$,

$$W(2\tau) = \cos(2\pi G_a \tau) \text{ for } H \parallel a: \theta = \frac{\pi}{2},$$
$$W(2\tau) = \cos(2\pi G_c \tau) \text{ for } H \parallel c: \theta = 0, \quad (2)$$

where θ is the angle between the c axis and magnetic field.

III. EXPERIMENT

Single crystals of $YbRh_2Si_2$ were grown with the ^{29}Si isotope enriched to $c = 52\%$, improving the NMR sensitivity by a factor ~11 by the In-flux method previously described [19]. High sample purity was confirmed by the small residual resistivity $\rho_0 \sim 0.99\ \mu\Omega$ cm and the large RRR value $=\rho(300\text{ K})/\rho(2\text{ K}) = 104$. No magnetic impurity phase was detected in magnetic susceptibility measurements. The antiferromagnetic phase transition was observed near 80 mK in zero field.

A single-crystal specimen ($6 \times 3 \times 0.1$ mm^3) was mounted in a ^{4}He cryostat with an NMR pickup coil. The present measurement has been done under an applied field $H = 7.2$ T. In $YbRh_2Si_2$, T_1 [19,20] and T_{2G} decrease with decreasing applied field. Thus, the applied field $H = 7.2$ T employed for the present study was chosen so that T_1 and T_{2G} would be long enough to allow precise determination of echo oscillation frequencies. Using a standard $\pi/2 - \pi$ pulse sequence, the spin-echo intensity $m(2\tau)$ so generated was measured as a function of the time τ between the pulses to record the spin-echo decay (see Figs. 2 and 3). Here, a typical $\pi/2$ pulse width was 4–5 μsec. Since the resonance linewidth is rather narrow (e.g., ~9 kHz at 7.2 T), all nuclear spins in the spectrum were quite uniformly excited by the radio frequency pulses used. The pulse repetition time $t_{rep}$was adjusted to be much longer than the previously determined T_1 [19,20].

Spin-echo oscillations due to RK and PD interactions occur if local inhomogeneous broadening is larger than the indirect RK and PD interactions [24]. This is clearly the case, since the observed inhomogeneous linewidth ~9 kHz at 7.2 T is much larger than the estimated $G_{a,c}$. Moreover, the echo

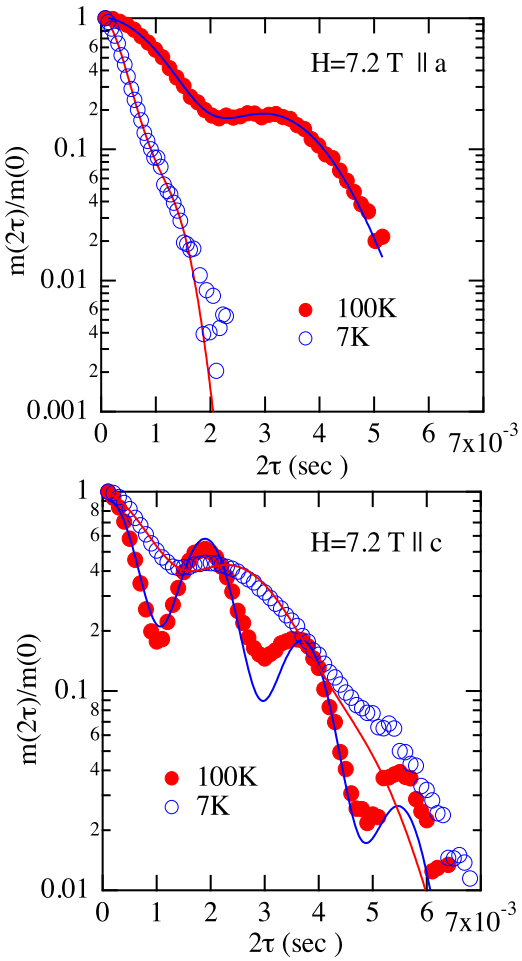

FIG. 3. 2τ dependence of $m(2\tau)/m(0)$ for $H \parallel a$ and c axes at 7 and 100 K. Solid lines are obtained using LS curve fitting for Eqs. (1) and (2). Previously measured T_1 values for $H \parallel a$ and c axes are adopted respectively here [19,20]. Parameters obtained from the fits, i.e., $1/T_{2Ga,c}$ and $G_{a,c}$, are presented in Fig. 5.

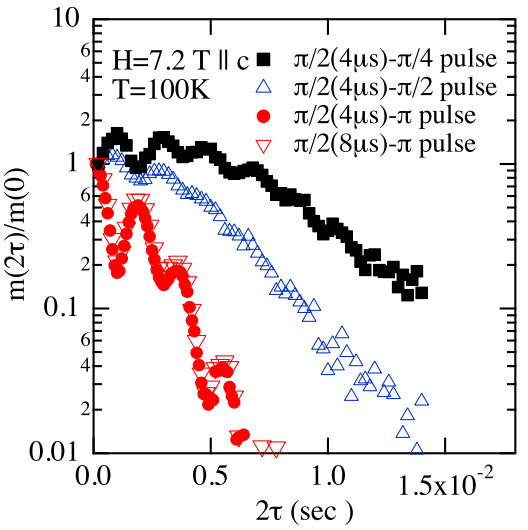

FIG. 4. Spin-echo decay curves with different pulse sequences for $H = 7.2$ T $\parallel c$ axis at 100 K. As the second pulse angle decreases, the spin-echo decay time becomes substantially longer, indicating that the spin-echo decay is static, i.e., driven by the rephasing pulse, aside from the T_1 process. For the $\pi/2 - \pi$ pulse sequence, the echo-decay curve is independent of pulse width ($8\mu s \geqslant \pi/2 \geqslant 4\mu s$), i.e., the strength of radio-frequency field, under conditions where all nuclei are uniformly excited.

relaxation process appears to be caused entirely by reversal of neighboring nuclear moments by the rephasing pulse. That is clear, because when the rephasing pulse angle is small (see Fig. 4), T_{2G} becomes very long. Thus, any genuinely dynamic transverse relaxation is very long, indeed.

IV. SPIN-ECHO DECAY RESULTS

A. T dependence of spin-echo decay

Figure 3 shows the spin-echo decay results for $YbRh_2Si_2$ with $H \parallel a$ and c axes. As shown in the figures, the experimental results can be fitted well using Eqs. (1) and (2), taking account of fractional occupation for ^{29}Si. The T dependence of G_a and G_c, as well as that of T_{2Ga} and T_{2Gc}, have been measured for $H \parallel a$ and $H \parallel c$, respectively. For this analysis, previously determined T_1 values for $H \parallel a$ and c axes have been adopted from [19] and [20], respectively.

Figure 4 shows spin-echo decay results with different refocusing-pulse angles for $H = 7.2$ T $\parallel c$ axis at 100 K. As the refocusing pulse width decreases, the spin-echo decay becomes slower, indicating that the spin-echo decay process is dominated by pulse modulation of static couplings, except for the (weak) T_1 relaxation process. In this situation, the echo is relaxed by the reorientation of neighbor spins by the refocusing (second) pulse [29]. These measurements confirm that the echo oscillations are not affected by other dynamical fluctuations, and T_{1L} can be replaced approximately by T_1. In addition, if the spin-echo intensity is optimized with a $\pi/2 - \pi$ sequence, the spin-echo decay curve is independent of pulse width, i.e., strength of radio-frequency field, on condition that all nuclei are uniformly excited (Fig. 4).

Figures 5(a) and 5(b) show the T dependence of $1/T_{2G}, G_{a,c}$. From $T = 300$ K down to $\sim$20 K, G_a and G_c are almost T independent. In contrast, a strong T dependence appears below 20 K, indicating that the indirect spin-spin coupling is T dependent at low temperatures. As the indirect nuclear spin-spin coupling is induced through (heavy) conduction bands, the present observation is naturally explained by a modification of electronic states at the Fermi level below 20 K.

Actually, a shoulder structure has been found below $\sim$20 K in the T dependence of the Hall coefficient [30]. In addition, for the Seebeck coefficient S, d^2S/dT^2 was reported to become negative below $\sim$20 K [31], also T dependence of $1/\tau(\omega)$ starts to deviate from the usual Drude behavior below 20 K in optical conductivity measurements [32]. The inset to Fig. 5(a) shows the T dependence of $1/T_1T$ below 100 K [19,20]. It seems that $d^2(1/T_1T)/dT^2 \sim d^2\mathrm{Im}\chi/dT^2$ also becomes negative below $\sim$20 K ($\mathrm{Im}\chi$ is the dissipative term of the dynamic susceptibility). These behaviors can be related to the observed modifications of $G_{a,c}$, as these coefficients are sensitive to the electronic state at the Fermi level. Further

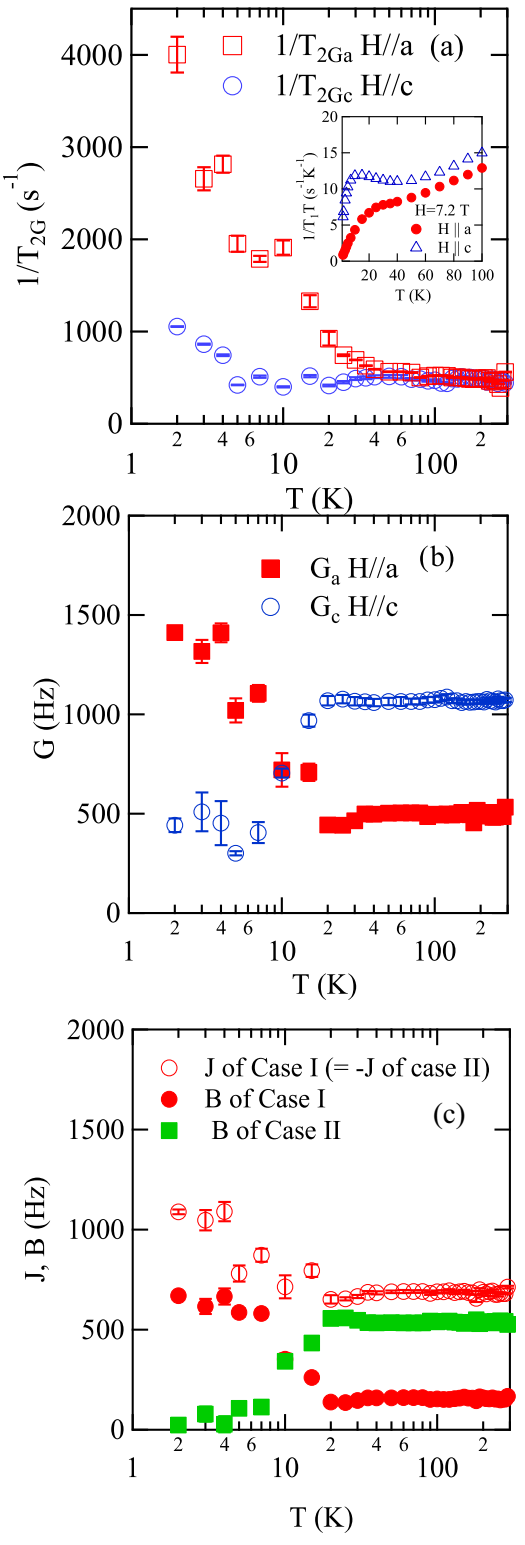

FIG. 5. T dependence of (a): $1/T_{2Ga,c}$; (b): $G_{a,c}$; (c): $J = \pm(2G_a + G_c)/3$ and $B = \pm(G_a - G_c)/3 + B_{cl}$ where double signs are coordinated. Although the sign cannot be determined, it is revealed that $|J|$ increases with decreasing T. Inset to (a): T dependence $1/T_1T$ for $H \parallel a,c$ axes.

discussion concerning modifications of the Fermi surface will be given in Sec. V.

B. T dependence of $1/T_{2G}$

As shown in Fig. 5(a), $1/T_{2G}$ increases with decreasing T, especially for the case of field $H \parallel a$. We suggest that temperature changes in $G_{a,c}$ should be accompanied by similar changes in the more distant coupling parameters [see $\tilde{J}_{0j}$ in Eq. (7)]. Because T_{2G} decay is driven by inversion of neighboring ^{29}Si spins by the refocusing pulse as in Fig. 4, we believe this process to be dominated by couplings with the 12 neighbor sites that lie within a range of 4 Å $\leqslant r_{0j} \leqslant$ 5 Å. These provide a distribution of couplings that are random in sign which, by the central limit theorem, yield an essentially Gaussian broadening effect. Such a distribution, when Fourier transformed, yields a result of the form of Eq. (1). With more detailed modeling of the indirect couplings, it should be possible to estimate T_{2G} in this fashion and relate its temperature dependence to that of $G_{a,c}$. In the meantime the form of this result is known, and its qualitative behavior is seen to be similar to that of G_a and G_c, as expected.

V. ANALYSIS BASED ON THE RK-PD MODEL

In this section, the observed T dependence of $G_{a,c}$ is interpreted based on the RK-PD model. At first, T dependence of RK interaction J and PD interaction B is estimated from $G_{a,c}$. Then the T dependence of J and B is assumed to be attributed to a modification of the Fermi surface. Based on this simplified picture, possible modification of the Fermi surface is discussed.

A. Modulation of the spin-echo decay ascribed to RK and PD interactions

It is well known that the RK and PD interactions can induce oscillations in the spin-echo decay curve [24,25]. In metals the indirect RK interaction between nuclear spins $\mathbf{I}_i, \mathbf{I}_j$ occurs through second-order scattering of conduction electrons [21], taking the scalar form

$$\mathcal{H}_J = \sum_{i>j} J_{ij} \mathbf{I}_i \cdot \mathbf{I}_j. \tag{3}$$

In addition and in contrast to the RK term, the PD interaction is a tensor quantity [25],

$$\mathcal{H}_B = \sum_{i>j} B_{ij} \left(\mathbf{I}_i \cdot \mathbf{I}_j - 3 I_j^z I_k^z \right), \tag{4}$$

$$B_{ij} = \tfrac{1}{2} b_{ij} (3\cos^2\theta_{ij} - 1), \tag{5}$$

where θ_{ij} is the angle between $\vec{r}_{ij}$ and the applied magnetic field, $\vec{r}_{ij}$ being the radius vector from the ith to the jth nucleus. b_{ij} is the effective coefficient for an indirect dipolar form of interaction B_{ij} between the ith and jth nuclear spins. Thus, the PD interaction depends on the direction of the applied field.

A complete formulation of the decay and modulation of free-induction and spin-echo signals has been given by Alloul and Froidevaux (AF) [25]. As will be demonstrated below, the T_2 process for this system is driven exclusively by nuclear-spin inversion of neighbor spins having significant spin-spin coupling, as described by (3) and (5). In such a case and with spins $I = 1/2$, the AF calculation gives the following *exact result* for the echo decay wave form of a nuclear spin "0" at

the origin.

$$m(2\tau) = \sum_{\lambda} \Pi_{j>0} \cos(2\pi \tilde{J}_{0j}\tau), \tag{6}$$

where index zero refers to the relaxing ^{29}Si spin at the origin, and $\sum_{\lambda}$ indicates a normalized sum over all configurations of neighbor spins given a concentration c of ^{29}Si, and where

$$h\tilde{J}_{0j} = J_{0j} + \left(b_{0j} - \hbar^2\gamma^2 r_{0j}^{-3}\right)(1 - 3\cos^2\theta_{0j}). \tag{7}$$

The second term in the parentheses is the classical dipole-dipole interaction between spins at the 0th and jth sites, which is of comparable magnitude to the PD coupling.

The first cosine factor in the indicated product in Eq. (6) represents the effect of ^{29}Si NN pairs in the $YbRh_2Si_2$ lattice, to which we ascribe all of the oscillatory behavior observed in our spin-echo decay data. We carry out the statistical sum over NN sites and introduce special parameter definitions for NN sites as follows: Thus, $hJ \equiv J_{01}$, $hB \equiv b_{01}$, $2\pi B_{cl} \equiv \hbar\gamma^2 R^{-3}$, $R \equiv r_{01}$, and $\theta \equiv \theta_{01}$, whereupon Eq. (6) can be rewritten as

$$m(2\tau) = \langle 2c^2\cos[2\pi\{J + (B - B_{cl})(1 - 3\cos^2\theta)\}\tau] + 2c(1 - c)\rangle \sum_{\lambda} \Pi_{j>1}\cos(2\pi \tilde{J}_{0j}\tau). \tag{8}$$

In the latter expression, the prefactor cosine term $\propto 2c^2$ describes oscillations from NN pairs that are expected to modulate the echo decay wave form, while the $2c(1 - c)$ term is the portion of the wave form from singly occupied pair sites that does not oscillate. The summation $\sum_{\lambda}$ describes the part of $m(2\tau)$ that is represented in Eq. (1) by the factor $\exp\{-0.5(2\tau/T_{2G})^2\}$. Below, the $2c^2$ term in the prefactor of Eq. (8) is fitted to spin-echo oscillation data to extract experimental values of J and B as a function of temperature. Meanwhile, the oscillatory modulation factor in Eq. (1) (square brackets) is identified as the quantity in angle brackets in Eq. (8) that includes the singly occupied NN pair sites that make no contribution to echo oscillations.

In this frame, the obtained $G_{a,c}$ [see Eq. (2)] of $YbRh_2Si_2$ may be expressed,

$$G_a = \pm\,(J + B - B_{cl})\colon \theta = \frac{\pi}{2},$$
$$G_c = \pm\,(J - 2B + 2B_{cl})\colon \theta = 0. \tag{9}$$

While technically there appear to be four possibilities in Eq. (9), physically only two are allowed, namely both (+) and both (−). Which of these is applicable can only be decided by other considerations, but is not required for a fit to our experimental data. The classical dipolar parameter B_{cl} is estimated to be 347 Hz using $R = 2.39$ Å in $YbRh_2Si_2$.

B. T dependence of J and B

As shown in Fig. 5(c), J and B are estimated using relations $J = \pm(2G_a + G_c)/3$ and $B = \pm(G_a - G_c)/3 + B_{cl}$ where the double signs are coordinated. There are two cases, case I where $J = (2G_a + G_c)/3$ and $B = (G_a - G_c)/3 + B_{cl}$, and case II, where $J = -(2G_a + G_c)/3$ and $B = (G_c - G_a)/3 + B_{cl}$. It should be noted that this behavior can be field dependent [12], though details of this effect are beyond the scope of this paper. For both cases I and II, $|J|$ increases with decreasing T. The amount of change of J and B below 20 K, i.e., $\Delta J \equiv |J(2\text{ K}) - J(20\text{ K})|$ and $\Delta B \equiv |B(2\text{ K}) - B(20\text{ K})|$, show a similar dependence on T, suggesting that the origin of these changes may be similar. In contrast, B increases for case I, but for case II it decreases with decreasing T. This difference is discussed below. In addition, $1/T_{2G}$ increases with decreasing T, indicating that changes of J and B lead to changes in the couplings $\tilde{J}_{0j}$ for more distant neighbors as well.

As J and B are sensitive to the character of the Fermi surface [22], the present results can be attributed to a modification of the Fermi surface below 20 K. In addition to the field-induced Lifshitz transition previously confirmed in $YbRh_2Si_2$ [11–13], one possible origin for this modification may be a temperature-induced Lifshitz transition, such as that observed, e.g., in WTe_2 [33].

On the other hand, modification of the Fermi surface due to a heavy quasiparticle band formation has been indicated below 50 K in previous ARPES measurements [18]. Thus, this heavy quasiparticle band formation is another possible origin for the modification of J and B. It is also consistent with the previously estimated Kondo temperature 25 K [31].

In contrast with the foregoing, no overall modification of the Fermi surface has been observed in recent ARPES measurements [17]. If the latter outcome holds up, then attribution of the observed T dependence of J and B to modifications of the Fermi surface would appear to contradict such a result. However, considering the following point, we think that there is not necessarily a contradiction here. The RK interaction between local Si sites is considered to occur via particular regions of the Fermi surface. Thus, the present results do not necessarily indicate an overall modification of the Fermi surface. The characteristics of such regions are discussed below.

C. Change of J and B due to Fermi-surface modification

The RK coupling J is related to electronic states at the Fermi level as follows [21,22]:

$$hJ = C_0\langle\Delta_0^2\rangle_{E_F} F_0(\boldsymbol{k_F}), \tag{10}$$

$$\Delta_0^2 \equiv u_k(\boldsymbol{r_i})u_{k'}^*(\boldsymbol{r_i})u_k(\boldsymbol{r_j})u_{k'}^*(\boldsymbol{r_j}) = u_k(\boldsymbol{r_i})^2 u_{k'}(\boldsymbol{r_i})^2, \tag{11}$$

$$F_0(\boldsymbol{k_F}) \equiv 2k_F R\cos(2k_F R) - \sin(2k_F R), \tag{12}$$

where $\boldsymbol{r_i}$ and $\boldsymbol{r_j}$ are NN Si sites; $e^{i\boldsymbol{kr}}u_k(\boldsymbol{r})$ is a typical Bloch function indexed by k; $\boldsymbol{k_F}$ is the Fermi wave vector; C_0 is a parameter that is considered to be nearly T independent (see the Appendix); $\boldsymbol{k}$ and $\boldsymbol{k'}$ are occupied and unoccupied states, respectively, near $\boldsymbol{k_F}$. As $\boldsymbol{r_i}$ and $\boldsymbol{r_j}$ are identical sites in the present case, Eq. (11) can be simplified. Δ_0^2 may correlate with the density of states at the Fermi level. $F_0(\boldsymbol{k_F})$ represents the oscillatory character of the RK interaction as shown in Fig. 6.

On the other hand for the parameter B, expansion of the Bloch states in spherical harmonics [34] may be useful. Thus,

$$u_k(\boldsymbol{r}) = u_k^0(\boldsymbol{r})P_0 + ikc_1u_k^1(\boldsymbol{r})P_1(\cos\theta_{\boldsymbol{kr}}) - k^2c_2u_k^2(\boldsymbol{r})P_2(\cos\theta_{\boldsymbol{kr}}) + \cdots, \tag{13}$$

$$P_l(\cos\theta_{\boldsymbol{kr}}) \equiv \Sigma_{m=-l}^{m=l}(-1)^m P_l^m(\cos\theta_{\boldsymbol{kr}}), \tag{14}$$

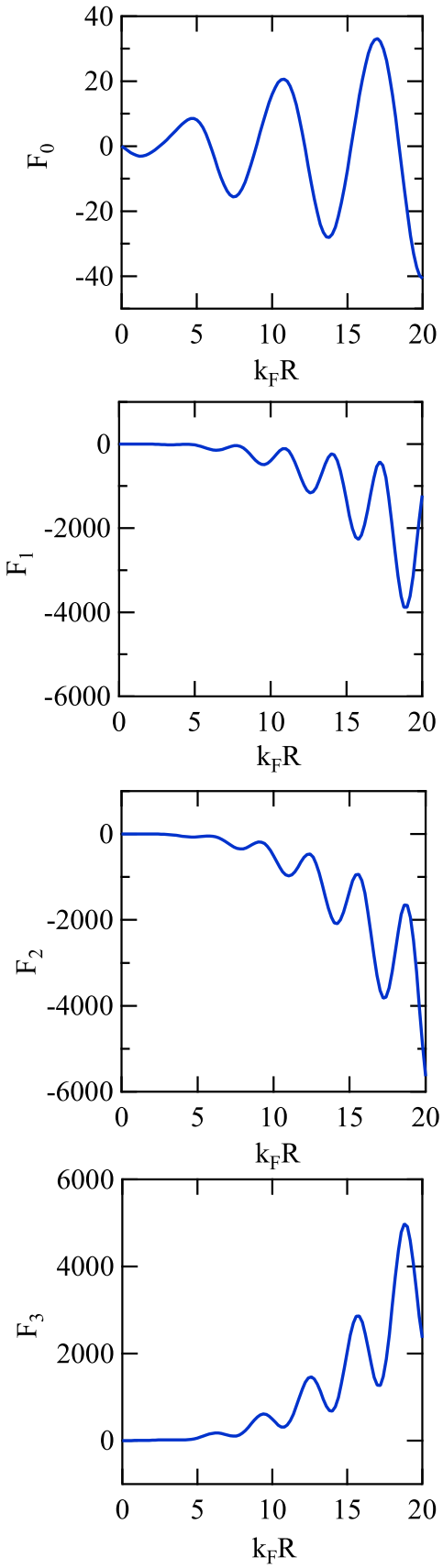

FIG. 6. $k_F R$ dependence of F_0, F_1, F_2, and F_3. F_0, i.e., the RK interaction, shows $\pm$ oscillation behavior. In contrast, F_1 and F_2 are negative but F_3 is positive regardless of $k_F R$.

where the $c_{1,2} > 0$ are constants determined near $k = 0$. P_l^m is the associated Legendre function; $\theta_{\boldsymbol{kr}}$ is the angle between $\boldsymbol{k}$ and $\boldsymbol{r}$; $u_k^l(\boldsymbol{r})$ is the coefficient for the P_l term ($P_0 = 1$). The P_0, P_1, and P_2 terms represent the s, p, and d orbital character of $u_k(\boldsymbol{r})$, respectively. Then B is expressed in terms of $u_k^1(\boldsymbol{r})$ and $u_k^2(\boldsymbol{r})$ as

$$hB = C_1\langle\Delta_p^2\rangle_{E_F} F_1(\boldsymbol{k_F}) + C_2\langle\Delta_{d1}^2\rangle_{E_F} F_2(\boldsymbol{k_F}) + C_3\langle\Delta_{d2}^2\rangle_{E_F} F_3(\boldsymbol{k_F}), \quad (15)$$

$$F_1(\boldsymbol{k_F}) \equiv \int_0^{k_F R} (\sin x - x\cos x)(\cos x - x\sin x)x\,dx, \quad (16)$$

$$F_2(\boldsymbol{k_F}) \equiv \int_0^{k_F R} \cos x\{(-x^2+3)\sin x - 3x\cos x\}x\,dx, \quad (17)$$

$$F_3(\boldsymbol{k_F}) \equiv \int_0^{k_F R} \sin x\{(-x^2+3)\cos x + 3x\sin x\}x\,dx, \quad (18)$$

$$\Delta_p^2 \equiv u_k(\boldsymbol{r_i})u_{k'}(\boldsymbol{r_i}) \int_0^{r_s} u_{k'}^{1*}(r)u_k^1(r)r^{-1}dr, \quad (19)$$

$$\Delta_{d1}^2 \equiv u_k(\boldsymbol{r_i})u_{k'}(\boldsymbol{r_i}) \int_0^{r_s} u_{k'}^{0*}(r)u_k^2(r)r^{-1}dr, \quad (20)$$

$$\Delta_{d2}^2 \equiv u_k(\boldsymbol{r_i})u_{k'}(\boldsymbol{r_i}) \int_0^{r_s} u_{k'}^{2*}(r)u_k^0(r)r^{-1}dr, \quad (21)$$

where r_s is the radius of the Wigner-Seitz sphere; C_{1-3} are constants which are considered nearly T independent (see the Appendix). It should be noted that estimates of C_{1-3} are beyond the scope of this paper.

Figure 6 shows the k_F dependence of $F_{1,2,3}(\boldsymbol{k_F})$. Regardless of k_F, F_3 is positive, whereas F_1 and F_2 are negative. As regards the T dependence of B for cases I and II, the positive third F_3 term in Eq. (15) becomes dominant, compared with the negative first (F_1) and/or second (F_2) terms in Eq. (15) below 20 K, or vice versa.

Although certain Fermi surfaces have not yet been observed in de Haas-van Alphen (dHvA) effect measurements at $T =$ 30 mK and field values above 16 T [16], the observed k_F is $= 1 \sim 3 \times 10^{10}$ m^{-1}, leading to $Rk_F = 2$–7. Even if this value of Rk_F is relevant for the present result, it is difficult to tell the sign of J from F_0 in Fig. 6 considering the uncertainty of the value of Rk_F. Nevertheless, if the overall Fermi surface is unchanged [17], the value of k_F, and thus the values of F_{0-3} are considered to be essentially unchanged in the paramagnetic state down to 70 mK. Therefore, the present T dependence for B can be attributed to the fact that the dominance among the Δ_{d2}^2, Δ_p^2, and Δ_{d1}^2 is T dependent below 20 K at 7.2 T for certain bands which give efficient contributions to the electron density of states at the Si site. As ΔJ and ΔB show similar T dependence, the T dependence of Δ_0^2 for $|J|$ may be due to the modifications of Δ_{d2}^2 and (Δ_p^2, Δ_{d1}^2), which is natural since Δ_0^2 correlates with the total density of states at the Fermi level.

At the Si site, Δ_p^2 may be mainly due to the atomic $2p$ orbital of Si; in contrast, hybridization between the $2s$,$2p$ orbitals of Si, $4d$ orbitals of Rh, and $4f$ orbitals of Yb is necessary to induce a $\Delta_{d1,2}^2$ term.

The present results can be attributed to that the Fermi surface that depends on these hybridizations has a T dependence

below 20 K. If heavy quasiparticle band formation [18] is the case, k_F can be T dependent, which can induce a modification of J and B in addition to the mechanism described above. At present, unfortunately, more concrete changes of the Fermi surface cannot be specified from this result.

Since the present measurements reflect the local electronic state at the Si site, the observed change of electronic state could be largely local. This may be only weakly sensed by k-space probes, since a local change might only correspond to a small modification over a broad region of k space. The absence of overall change of Fermi surface in the ARPES measurements [17] could be explained by this picture. In fact, the Fermi surface seems to appear differently, depending on the experimental probe up to now. This sort of complexity could be partly due to such a particular nearly localized state.

LDA band calculations could not well reproduce the dHvA measurements [16], which may be consistent with a possible nearly localized electronic state of $YbRh_2Si_2$, since the simple LDA method is not ideal for a localized state. In order to clarify this situation, a comparison of experimental results with a calculated T dependence for the bands using, e.g., advanced DMFT methods [35] may be quite useful, since the T dependence of $\Delta^2_{0,p,d1,d2}$ could then be discussed quantitatively.

VI. CONCLUSION

The ^{29}Si nuclear spin-echo oscillations and T_{2G} show clear strong T dependence at low temperatures in $YbRh_2Si_2$, indicating that the electronic state at the Fermi level starts to change below 20 K. This energy scale is consistent with other previous measurements, which may be characterized by the Kondo temperature 25 K. However, the corresponding change of Fermi surface may be peculiar in $YbRh_2Si_2$ due to a nearly localized electronic state, which is considered to be related with the possibly exotic QCPT. As the observed spin-echo decay curve can be explained by the RK-PD model, the description via the RK-PD model appears to be valid for a heavy fermion system.

ACKNOWLEDGMENTS

We are grateful for stimulating discussions with H. Harima, D. Aoki, and K. Izawa. This work was supported by JSPS KAKENHI Grants No. 15H05884 (J-Physics) and No. 15K05152 and the REIMEI Research Program of JAEA.

APPENDIX

The constants in Eqs. (10) and (15) are expressed as follows [22]:

$$C_0 \equiv \frac{m'}{2^5\pi^3\hbar^2R^4}\left(\frac{16\pi g_N\beta_N\beta}{3}\right)^2, \tag{A1}$$

$$C_1 \equiv \frac{8m'c_1c_1'}{15\pi^2\hbar^2R^6}\frac{16\pi g(g_N\beta_N\beta)^2}{3}, \tag{A2}$$

$$C_2 \equiv \frac{c_2}{4c_1c_1'}C_1, \tag{A3}$$

$$C_3 \equiv \frac{c_2'}{c_2}C_2, \tag{A4}$$

where m' is the effective cyclotron mass of the electron; g_N and g are the g values of nuclei and electrons, respectively; β and β_N are the electron and nuclear Bohr magnetons, respectively; the $c'_{1,2}$ are constants in Eq. (13) for the $u_{k'}$ state. If we take m' to be the electron rest mass, C_0 is found to be 2×10^{-30} J $\sim 3\times10^3$ Hz. Then, for tentative reasonable values $|F_0|=1$ and $\langle\Delta_0^2\rangle_{E_F}=0.1$, $|J|=C_0|F_0|\langle\Delta_0^2\rangle_{E_F}$ is found to be $\sim 3\times10^2$ Hz, which is comparable with the observed $|J|$. On the other hand, C_{1-3} cannot be estimated, since $c_{1,2}$ and $c'_{1,2}$ are unknown.

[1] T. Moriya and T. Takimoto, J. Phys. Soc. Jpn. **64**, 960 (1995).
[2] A. J. Millis, Phys. Rev. B **48**, 7183 (1993).
[3] P. Gegenwart, Q. Si, and F. Steglich, Nat. Phys. **4**, 186 (2008).
[4] Q. Si, S. Rabello, K. Ingersent, and J. L. Smith, Nature (London) **413**, 804 (2001).
[5] P. Coleman, C. Pépin, Q. Si, and R. Ramazashvili, J. Phys.: Condens. Matter **13**, R723 (2001).
[6] E. Abrahams, J. Schmalian, and P. Wölfle, Phys. Rev. B **90**, 045105 (2014).
[7] S. Paschen, T. Lühmann, S. Wirth, P. Gegenwart, O. Trovarelli, C. Geibel, F. Steglich, P. Coleman, and Q. Si, Nature (London) **432**, 881 (2004).
[8] S. Friedemann, T. Westerkamp, M. Brando, N. Oeschler, S. Wirth, P. Gegenwart, C. Krellner, C. Geibel, and F. Steglich, Proc. Natl. Acad. Sci. USA **107**, 14547 (2010).
[9] J. Custers, P. Gegenwart, H. Wilhelm, K. Neumaier, Y. Tokiwa, O. Trovarelli, C. Geibel, F. Steglich, C. Pépin, and P. Coleman, Nature (London) **424**, 524 (2003).
[10] H. Pfau, S. Hartmann, U. Stockert, P. Sun, S. Lausberg, M. Brando, S. Friedemann, C. Krellner, C. Geibel, S. Wirth, S. Kirchner, E. Abrahams, Q. Si, and F. Steglich, Nature (London) **484**, 494 (2012).
[11] Y. Machida, K. Tomokuni, C. Ogura, K. Izawa, K. Kuga, S. Nakatsuji, G. Lapertot, G. Knebel, J.-P. Brison, and J. Flouquet, Phys. Rev. Lett. **109**, 156405 (2012).
[12] A. Pourret, G. Knebel, T. D. Matsuda, G. Lapertot, and J. Flouquet, J. Phys. Soc. Jpn. **82**, 053704 (2013).
[13] H. R. Naren, S. Friedemann, G. Zwicknagel, C. Krellner, C. Geibel, F. Steglich, and S. Wirth, New J. Phys. **15**, 093032 (2013).
[14] G. Zwicknagel, J. Phys.: Condens. Matter **23**, 094215 (2011).
[15] P. M. C. Rourke, A. McCollam, G. Lapertot, G. Knebel, J. Flouquet, and S. R. Julian, Phys. Rev. Lett. **101**, 237205 (2008).
[16] G. Knebel, R. Boursier, E. Hassinger, G. Lapertot, P. G. Niklowitz, A. Pourret, B. Salce, J. P. Sanchez, I. Sheikin, P. Bonville, H. Harima, and J. Flouquet, J. Phys. Soc. Jpn. **75**, 114709 (2006).
[17] K. Kummer, S. Patil, A. Chikina, M. Güttler, M. Höppner, A. Generalov, S. Danzenbächer, S. Seiro, A. Hannaske, C. Krellner, Yu. Kucherenko, M. Shi, M. Radovic, E. Rienks, G. Zwicknagl,

K. Matho, J. W. Allen, C. Laubschat, C. Geibel, and D. V. Vyalikh, Phys. Rev. X **5**, 011028 (2015).
[18] S.-K. Mo, W. S. Lee, F. Schmitt, Y. L. Chen, D. H. Lu, C. Capan, D. J. Kim, Z. Fisk, C.-Q. Zhang, Z. Hussain, and Z.-X. Shen, Phys. Rev. B **85**, 241103(R) (2012).
[19] S. Kambe, H. Sakai, Y. Tokunaga, G. Lapertot, T. D. Matsuda, G. Knebel, J. Flouquet, and R. E. Walstedt, Nat. Phys. **10**, 840 (2014).
[20] S. Kambe, H. Sakai, Y. Tokunaga, G. Lapertot, T. D. Matsuda, G. Knebel, J. Flouquet, and R. E. Walstedt, Phys. Rev. B **91**, 161110(R) (2015).
[21] M. A. Ruderman and C. Kittel, Phys. Rev. **96**, 99 (1954); it should be noted that the RK interaction between nuclear moments here is different from the Ruderman-Kittel-Kasuya-Yosida (RKKY) interaction between electron magnetic moments.
[22] N. Bloembergen and T. J. Rowland, Phys. Rev. **97**, 1679 (1955).
[23] R. E. Walstedt, M. W. Dowley, E. L. Hahn, and C. Froidevaux, Phys. Rev. Lett. **8**, 406 (1962).
[24] C. Froidevaux and M. Weger, Phys. Rev. Lett. **12**, 123 (1964).
[25] H. Alloul and C. Froidevaux, Phys. Rev. **163**, 324 (1967).
[26] N. M. Georgieva, D. Rybicki, R. Guehne, G. V. M. Williams, S. V. Chong, K. Kadowaki, I. Garate, and J. Haase, Phys. Rev. B **93**, 195120 (2016).
[27] K. Ishida, K. Okamoto, Y. Kawasaki, Y. Kitaoka, O. Trovarelli, C. Geibel, and F. Steglich, Phys. Rev. Lett. **89**, 107202 (2002).
[28] S. Kambe, H. Sakai, Y. Tokunaga, G. Lapertot, T. D. Matsuda, G. Knebel, J. Flouquet, and R. E. Walstedt, J. Phys. Conf. Ser. **683**, 012006 (2016).
[29] R. E. Walstedt and S-W. Cheong, Phys. Rev. B **51**, 3163 (1995).
[30] S. Friedemann, S. Wirth, N. Oeschler, C. Krellner, C. Geibel, F. Steglich, S. MaQuilon, Z. Fisk, S. Paschen, and G. Zwicknagl, Phys. Rev. B **82**, 035103 (2010).
[31] U. Köhler, N. Oeschler, F. Steglich, S. Maquilon, and Z. Fisk, Phys. Rev. B **77**, 104412 (2008).
[32] S. Kimura, J. Sichelschmidt, J. Ferstl, C. Krellner, C. Geibel, and F. Steglich, Phys. Rev. B **74**, 132408 (2006).
[33] Y. Wu, N. H. Jo, M. Ochi, L. Huang, D. Mou, S. L. Bud'ko, P. C. Canfield, N. Trivedi, R. Arita, and A. Kaminski, Phys. Rev. Lett. **115**, 166602 (2015).
[34] J. Bardeen, J. Chem. Phys. **6**, 367 (1934).
[35] G. Kotliar, S. Y. Savrasov, K. Haule, V. S. Oudovenko, O. Parcollet, and C. A. Marianetti, Rev. Mod. Phys. **78**, 865 (2006).